JOURNAL OF MATERIALS SCIENCE 31 (1996) 4303–4306

In situ laser surface coating of TiC metal–matrix composite layer

MENG YAN, HU HANQI
Department of Metallurgy, Science and Technology, University Beijing, People's Republic of China

Surface alloys are of great interest for improving the mechanical and/or chemical properties of the near-surface region on metallic materials. A new method, *in situ* laser surface coating of metal–matrix composite, is described, by which to produce a surface composite layer. Using this process, γ-Ni–TiC_x composite surface layers were achieved on mild steel; they exhibited increased hardness, and *in situ* formed TiC_x particles, 0.5–0.8 μm in size, were homogeneously distributed in the top half of the matrix layer.

1. Introduction

The use of laser cladding and alloying allows the coating layer or the surface region metals to be modified by addition of a foreign material. Such modifications can lead to a surface composite where the foreign material precipitates within the cladding metallic matrix. The composite structure, appearing when the solubility of the foreign material is low, is frequently observed in the case of carbide or nitride additions to metals. It can afford improved hardness and wear resistance to the base metal [1], depending on the volume fraction incorporated. As an example, in automative internal combustion engine pistons, where enhanced wear resistance and desirable frictional properties are needed, a dispersion of silicon carbide in the aluminium matrix is gradually being adopted in the place of unreinforced alloy [2]. Among other composites of this type already studied and reported in the literature, are Co/WC–TiC and Ni–TiC [3].

Different methods of preparation of such composites have been reported: precipitation from Fe–Ti–C melt of appropriate composition [4]; sintering of TiC powders with iron [5]; chemical vapour deposition of TiC [6], or laser mixing of evaporated films of Fe–Ti–C [7]. Of particular importance in this area of study is the work of Ayers *et al.* [8] who used a particle injection method. This method was justified by the large difference between the volume mass of titanium carbide and that of stainless steel; these authors claimed that without injection, it simply floats on top of the melt pool unless it enters it with sufficient velocity. Unfortunately, the Fe–TiC composites obtained by this method were never crack-free. More recently, Ceri *et al.* [9] and Ariely *et al.* [10] have produced a carbide-reinforced layer by the TiC laser-injection technique. In contrast to Ayers *et al.* [8], the coating was defect-free. Kim and Seong [11] have studied Fe–TiN material from a slurry of TiN particles in propyl alcohol, deposited on to iron and irradiated under different power densities with argon or nitrogen as the shielding gas. The authors claimed that a fraction of the TiN decomposed to titanium and nitrogen under an argon atomosphere, whereas no decomposition occurred under nitrogen. Fasasi *et al.* [12] produced Fe–TiC crack-free surface composites on mild steel by laser irradition of a mixture of submicrometre TiC particles and polyethyleneglycol deposited on the metallic substrate.

For composites, the main strengthening mechanism is transfer of stress from the matrix to the reinforcement phase through a shear mechanism. At elevated temperatures, effective stress transfer does not occur, owing to softening of the matrix resulting from precipitate coarsening. Therefore, the elevated temperature strength of such composites is not satisfactory, and the scope of application is reduced. In more recent years, a novel approach the *in situ* metal–matrix composite method, has been studied to prepare composite materials. In this method, reinforcements were introduced into the metal matrix by the reaction between the added particles or melt, such *in situ* formed reinforced particles, including TiB_2 [13], TiC [14, 15] and Al_4C_3 [16, 17], may be more compatible with the matrix and the interfaces may be cleaner [18] as compared to the composites produced conventionally. Meanwhile, because the *in situ* formed precipitates are often ultra-fine particles, the elevated temperature strength of these composites would be raised, because the *in situ* formed dispersoids are thermally stable and ensure that the composite matrix has sufficient strength to transfer stress. The *in situ* composites exhibit improved strength retention at elevated temperatures, and useful increases in wear and fatigue resistance [16, 19].

The aim of the present investigation was to form *in situ* TiC dispersoid in nickel-based laser cladding layer on mild steel substrate using a new original method (*in situ* laser surface composite coating) to improve the hardness, wear and fatigue resistance and the elevated temperature strength of the composite layer. Such an investigation has not been reported previously in the literature.

0022–2461

TABLE I Size and purity of the element powders

Element	Size (mesh)	Purity (wt %)	Content (wt %)
Ni60A	− 200	–	90
Ti + C $\left(\frac{Ti}{C}\right)$	− 320	99.9	10
	− 320	99.5	

2. Experimental procedure

Elemental powders of various sizes were mixed to obtain mixed powder in the desirable condition. Table I shows the size and purity of the element powder. Ni60A was commercially available self-melted alloy powder, with chemical composition 16 wt % Cr, 3.5 wt % B, 4.5 wt % Si, 0.8 wt % C, balance nickle, with nominal hardness HRc60 (Hv690), and tested by us in laser cladding.

A 2.5 kW CO_2 laser operated at 1.5–2.0 kW with a 3–5 mm beam diameter was used for laser cladding. The key variables that control efficiency of laser surface processing are laser power, beam size, and scan speed; they determine the extent of surface cladding, coating composition and coating thickness. The traverse speed of the substrate (commercial mild steel) relative to the laser beam was varied between 3 and 10 mm s^{-1}; the mixed powders were prepared on the surface (0.5–1.2 mm). The process was carried out under an effective shroud of nitrogen gas to minimize contamination and oxidization of the laser-melted region. After laser cladding, a transverse section was produced. Optical microscopy, scanning election microscopy (SEM) with energy dispersive spectroscopy (EDS) were used for the microstructural and compositional examination. The phases of the coating were analysed by X-ray diffraction (XRD). A D_{max}-RB 12 kW diffractometer was used to define layer phases. The radiation was CuK_α with working voltage and current of 40 kV and 120 mA, respectively. The step speed was 5° min^{-1}. The microhardness was measured on a section perpendicular to the treated surface from the surface inwards, with a load of 200 g.

3. Results and discussion

Fig. 1 shows a micrograph of a cross-section of the treated zone produced from a mixture containing 10 wt % (Ti + C) + 90 wt % Ni60A, using a 1.9 kW laser powder, a 4 mm beam diameter, a 5 mm s^{-1} traverse speed and an overlap of 20%. The track thickness (distance from the top surface of the layer to the interface with the substrate) was 0.9 mm. Some porosity, within the pore-size range 10–50 μm (diameter) was observed. Such porosity decreases when the specimen was preheated before cladding and when the layer is thinner. Cracks were not observed on the surface of all the tracks. The surface roughness is slight relative to the depth of the layer.

Fig. 2 shows the XRD spectrum taken at 0.3 mm depth. The X-ray examinations showed that the phase was composed of γ–Ni, TiC_x, Ni_5Si_2, Cr_{23} (C, B)$_6$, and Cr_2B. In the diffraction pattern taken at different depths in zones parallel to the surface, no intermetallic phases characteristic of the binary system Ni–Ti could be detected.

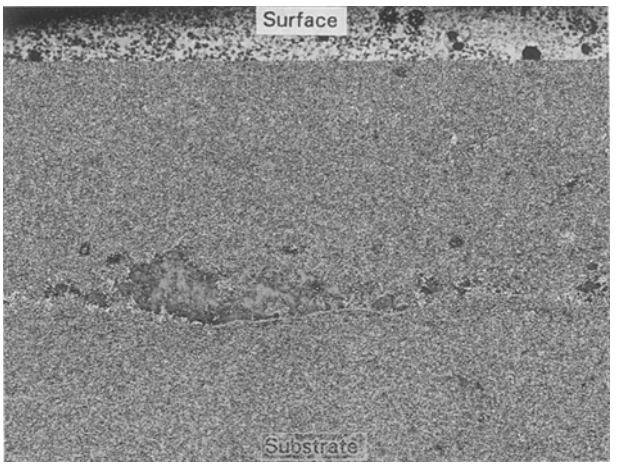

Figure 1 Micrograph of the layer cross-section.

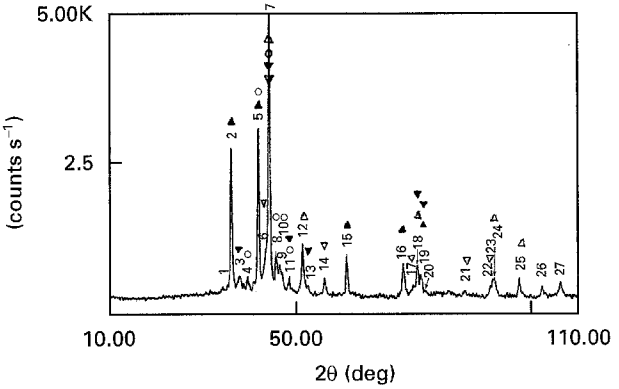

Figure 2 X-ray spectrum taken at 0.3 mm depth in the LSC zone. (△) γ-Ni, (▲) TiC_x, (▽) Cr_2B, (▼) $Cr_{23}C_6$, (○) Ni_5Si_2.

The carbide and nitride of titanium have cubic NaCl-type crystal structures and are completely soluble in each other [20]. Both TiC and TiN phases exist over a wide range of stoichiometric ratios (with $x = 0.5$–1). In principle, in a nitrogen atmosphere, the formed titanium carbide should be accompanied by titanium nitride. However, for any given nitrogen pressure, an increase in temperature favours the formation of TiC_x. Experimental results of temperature and pressure under which a self-propagating reaction can be sustained, as plotted by Eslamloo-Grami and Munir [20], are shown in Fig. 3. In the

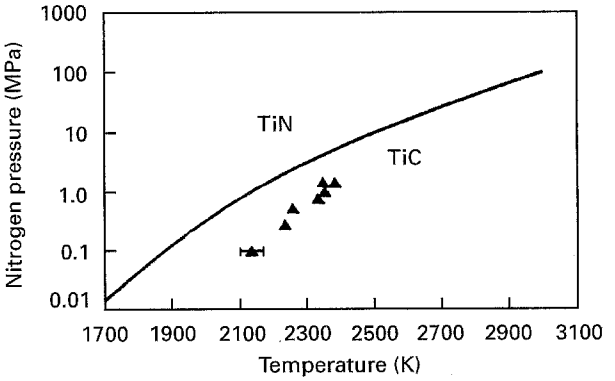

Figure 3 Stability regions for TiC and TiN. (▲) Experimental minimum combustion temperatures.

TABLE II The measurements on the crystal planes and the lattice parameters of TiC_x at different depths

Distance from layer surface (mm)	Measurements of different planes			Lattice parameters (Å) (based on (0 0 2) plane)
	(0 0 2)	(1 1 1)	(2 2 0)	
0.15	2.150	2.479	1.521	4.300
0.30	2.159	2.491	1.524	4.318
0.45	2.163	2.494	1.528	4.326

cases under the laser cladding processes, at 2000–2500 K, the carbide phase is more thermodynamically favoured than the nitride phase. However, because the reactions are not under equilibrium conditions, there may be some nitride disolved in the TiC_x to form carbonitrides, TiC_xN_y. To verify the phenomenon, another set of XRD patterns at different depths from the surface, was obtained. Table II gives the measurements on the crystal planes of TiC_xN_y. The lattice parameters (based on X-ray measurements on the (0 0 2) planes) near the top of the layer, are somewhat smaller than those at increasing distance from the surface. The parameters increase towards the value corresponding to the increase of carbon content or the decrease of nitrogen content [20]. This could be ascribed to the oxidization of carbon or the formation of the carbonitride in the top zone near the layer surface. If the effect of nitride was removed, the value of x in TiC_x varied from 4.310–4.326, which means x varied nearly from 0.6–0.9. Table III [20, 21] gives the relation between x and lattice parameters.

Microhardness measurements as a function of depth were carried out on polished cross-sections of the surface composites with a Vickers indentor at a load of 200 gf. The results in Fig. 4, show that the hardness at a depth of about 150 μm is considerably higher than that of the surface. At a depth of about 450 μm, where the TiC_x fraction decreases sharply, the hardness also drops. At a depth of about 900 μm, where the layer that has been melted ends and the heat-affected zone (HAZ) begins, the hardness again drops sharply. From here it decreases steadily until the hardness of the substrate (about 120 H_v) is reached at a depth of about 1.6 mm. The hardness profile includes measurements on the TiC_x particles themselves, which is the reason why the size of 0.5–0.8 μm cannot affect the measurements of 200 gf.

Fig. 5a–d shows the microstructure of the various subzones in the cross-section of the treated layer, shown in Fig. 1 which have different hardness values. Fig. 5a depicts the zone at about the 0.1–0.3 mm depth. The identified TiC_x particles, thick needle-shaped or irregular grains, are homogeneously distributed at a depth of 0–450 μm from the surface. This can be ascribed to the low weight of titanium, carbon and TiC_x. At a depth of about 250–450 μm, there are some

TABLE III Relation between carbon content and lattice parameter of TiC_xN_y

	$TiC_{0.5}N_{0.5}$	$TiC_{0.5}$	$TiC_{0.605}$	$TiC_{0.775}$	$TiC_{0.976}$
Lattice parameter (Å)	4.2830	4.3025	4.3142	4.3253	4.3278

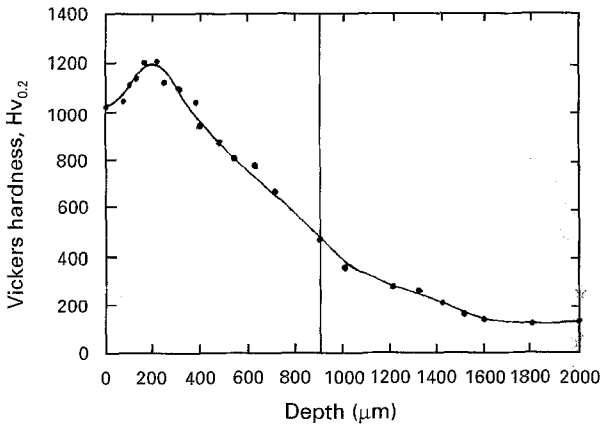

Figure 4 Vickers microhardness as a function of depth.

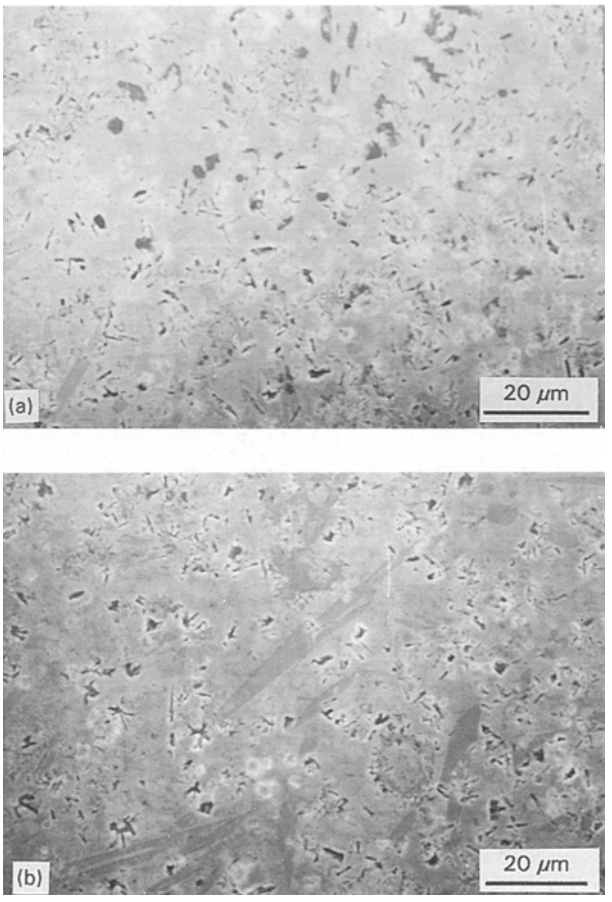

Figure 5 Detailed photomicrographs of a cross-section of the LAS zone. (a) Surface zone (zone 1 in Fig. 1); (b) half-depth of the layer (zone 2 in Fig. 1); (c) bottom of the molten bath (zone 3 in Fig. 1); (d) the interface between the layer and the substrate.

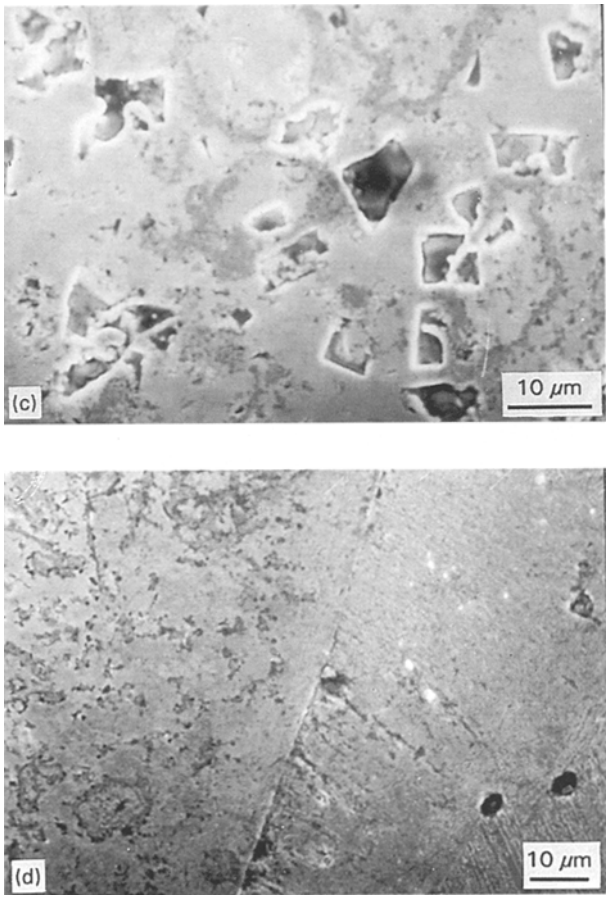

Figure 5 Continued.

needle-shaped grains identified as $Cr_{23}(C, B)_6$, shown in Fig. 5b. At 450–900 μm, the main phases are γ–Ni with some regular-shaped Ni_5Si_2 shown in Fig. 5c. The maximum hardness, measured at a depth of 100–200 μm from the surface indicates a higher carbon content in TiC_x or the carbontride phase at the zone near the surface, than in the layer surface itself. At the bottom of the melted zone, some regular-shaped Cr_2B phase can be seen. These microstructures correspond to the hardness profile, as can be seen by comparing Figs 1, 4 and 5. The interface between the cladding layer and the substrate is shown in Fig. 5d.

4. Conclusion

The new and original method of *in situ* laser surface coating of a TiC_x metal–matrix composites layer has been successfully applied to prepare γ-Ni–TiC surface composites on mild steel. The reinforcement particles, TiC_x, were introduced by adding titanium and graphite, which reacted to form TiC_x during the laser cladding process, rather than TiC particles being introduced into the melted zone directly. The main advantage of the proposed technique was the *in situ* formed submicrometre TiC_x particles in the layer. It is well known that the volume fraction, particle size and the interface between particle and matrix and the uniformity of the dispersion can affect signficantly the mechanical properties of the materials. The *in situ* formed γ-Ni–TiC composite layer, because of the homogeneous distribution of TiC particles, uncontaminated TiC surface and 0.5–0.8 μm size, could be expected to have good heat and wear resistance and other mechanical properties.

After solidification, the resulting surface composites are composed of γ-Ni, TiC_x, $Cr_{23}C_6$ Ni_5Si_2 and Cr_2B phases. The top half of the layer is mainly composed of γ–Ni and TiC_x. This microstructure is in a good agreement with the microhardness. The highest hardness at a depth of 150–200 μm is high: 1200 $H_{v0.2}$. The underlying mechanisms (the reaction mechanism of titanium and carbon, the microstruction of TiC_x, and carbon content of TiC, etc. have not been studied fully. However, it is believed that the composite structure obtained, its homogeneity over large dimensions, and the absence of cracks even after rapid solidification, could lead to improved bonding between TiC_x and matrix and improved wear performance of the substrate. Further studies will be conducted on these mechanisms, and the tribological properties of the described coatings at high temperature will be compared with those achieved by the laser composite technique. The conventional production of such coatings will be extended towards industrial alloys.

References

1. W. A. GLAESER, "Materials for tribology" Tribology Series 20 (Elsevier, Amsterdam, 1992) pp. 8–45.
2. B. DE CELLIS, *Wear* **116** (1987) 298.
3. A. BACHLI and A. BLATTER, *Surf. Coat. Technol.* **45** (1991) 397.
4. T. Z. KATTAMIS and T. SUGANAMA, *Mater. Sci. Eng.* **A128** (1990) 241.
5. K. W. CHAE, D. CHUN, D. KIM, Y. BAIK and K. Y. EWN, *J. Am. Ceram. Soc.* **73** (1990) 1979.
6. P. P. RAMAEKERS, F. J. J. VAN LOO and G. F. BASTING, *Z. Metallkde.* **76** (1985) 245.
7. M. NASTASI, J. P. HIRVONEN, T. G. ZOCCO and T. R. JERVIS, *J. Mater. Res.* **5** (1990) 1207.
8. J. D. AYERS and T. R. TUCKER, *Thin Solid Films* **73** (1980) 201.
9. W. CERI, R. MARTINELLA, G. P. MOR, P. BIANCHI and D. D. ANGELO, *Surf. Coat. Technol.* **49** (1991) 40.
10. S. ARIELY, J. SHEN, M. BAMBERGER, F. DANSIGER and H. HUGEL, *Surf. Coat. Technol.* **45** (1991) 403.
11. T. H. KIM and B. G. SEONG, *J. Mater. Sci.* **25** (1990) 3583.
12. A. Y. FASASI, M. PONS, C. TASSIN, A. GALERIE, C. SAINFORT and C. POLAK, *ibid.* **29** (1994) 5121.
13. T. J. LANGAN and J. R. PICKENS, *Scripta Metall. Mater.* **25** (1991) 1587.
14. G. M. VYLETEL, D. C. VAN AKEN and M. E. ALLISON, *ibid.* **25** (1991) 2405.
15. R. MITRA, W. A. CHIOU, J. R. WEERTMAN and M. E. FINE, *ibid.* **25** (1991) 2689.
16. V. ARNHOLD and J. BAUMGARTEN, *Powder Metall. Int.* **17** (1985) 168.
17. J. BI, Z. Y. MA, S. J. WU, Y. X. LU and H. W. SHEN, *J. Mater. Sci. Technol.* **9** (1993) 61.
18. D. LEWIS III, in "Metal matrix Composits: Processing and Interface", edited by R. K. Everett and R. J. Arsenault (Academic Press, San Diego, 1991) p. 141.
19. A. R. C. WESTWOOD, *Metall. Trans.* **19A** (1988) 749.
20. M. ESLAMLOO-GRAMI and Z. A. MUNIR, *J. Mater. Res.* **9** (1994) 431.
21. WANG GODONG, "Production Theory of Hard Alloy, Metallurgy", 1st Edn (Industry Press, Beijing, 1988) p. 85.

Received 8 August
and accepted 21 December 1995